Infection characteristics among *Serratia marcescens* capsule lineages.

running title: differentiating *S. marcescens* capsule types

Mark T. Anderson[a]#, Stephanie D. Himpsl[a], Leandra G. Kingsley[a]*, Sara N. Smith[a]$, Michael A. Bachman[a,b], and Harry L. T. Mobley[a]

[a] University of Michigan, Michigan Medicine. Department of Microbiology and Immunology. Ann Arbor, MI U. S. A.

[b] University of Michigan, Michigan Medicine. Department of Pathology. Ann Arbor, MI U. S. A.

* present address: Stanford University, Department of Pathology. Stanford, CA U. S. A.

$ present address: University of Michigan, Michigan Medicine. Department of Anesthesiology. Ann Arbor, MI U. S. A.

address correspondence to Mark T. Anderson: andersma@umich.edu

Abstract: 244 words

Importance: 115 words

Text: 4,970 words

ABSTRACT

Serratia marcescens is a healthcare-associated pathogen that causes bloodstream infections, pneumonia, and urinary tract infections. The capsule polysaccharide of *S. marcescens* is a critical fitness determinant during infection and recent work established the relationship between capsule locus (KL) genetic sequences within the species. Strains belonging to KL1 and KL2 capsule clades produce sialylated polysaccharides and represent the largest subpopulation of isolates from clinical origin while the *S. marcescens* type strain and other environmental isolates were classified as KL5. In this work, the contribution of these and other capsules to pathogenesis in multiple infection models was determined. Using a murine tail vein injection model of bacteremia, clinical strains demonstrated capsule-dependent colonization of spleen, liver, and kidney following inoculation. The KL5 strain, in contrast, exhibited no loss of survival in this model when capsule genes were deleted. Furthermore, the wild-type KL5 strain was cleared more rapidly from both the spleen and liver compared to a KL1 strain. Similar results were observed in a bacteremic pneumonia model in that all tested strains of clinical origin demonstrated a requirement for capsule in both the primary lung infection site and for bloodstream dissemination to other organs. Finally, strains from each KL clade were tested for the role of capsule in internalization by bone marrow-derived macrophages. Only the sialylated KL1 and KL2 clade strains, representing the majority of clinical isolates, exhibited capsule-dependent inhibition of internalization, suggesting that capsule-mediated resistance to macrophage phagocytosis may enhance survival and antibacterial defenses during infection.

IMPORTANCE

Bacterial bloodstream infections result from evasion of the host innate immune system and stable colonization following an initial inoculation event from either an internal or external source. Capsule polysaccharides play a protective role for *Serratia marcescens* during bacteremia but there is abundant genetic diversity at the capsule-encoding locus within the species. This study

compares the infection characteristics of *S. marcescens* isolates belonging to five different capsule types and defines the contributions to infection fitness for each type. By characterizing the differences in capsule dependence and infection potential between *S. marcescens* strains, efforts to combat these life-threatening infections can be focused toward identifying strategies that target the most critical genetic lineages of this important opportunistic pathogen.

INTRODUCTION

Serratia marcescens is one of several commonly identified causes of bacteremia and pneumonia among Gram-negative bacterial species (1, 2) and an estimated 100,000 deaths (42,000 associated with drug resistance) were due to *Serratia* species in 2019 alone (3, 4). Many of these infections occur in individuals with pre-existing conditions or during prolonged hospital stays. Pediatric populations are also vulnerable to severe *S. marcescens* infections as evidenced by the numerous nosocomial outbreaks and their consequences that are described in the literature (5-7). In addition to the systemic and life-threatening infections that are the focus of this work, *S. marcescens* is capable of a wide range of other pathogenic interactions with both human and non-human hosts (8-11). The clinical significance of *S. marcescens* is also contrasted by the prevalence with which this species is found in other environments, with isolation sources ranging from soil, water, plants, and insects (8) and highlighting the range of niches in which the organism thrives.

Genomic studies investigating the population structure of *Serratia marcescens* published in the last several years have defined the species-level diversity for this opportunistic pathogen and, when considered broadly, have reached similar conclusions regarding the delineation of genetically-distinct clades within the species. First, certain lineages have stringent correlations with clinical sources, consistent with niche adaptation to the infection environment for a subset of genotypes and supported by a discrete repertoire of accessory genomic elements enriched within these clades (12-15). The converse relationship is also observed in that other lineages within the species are highly associated with non-clinical or environmental sources. Furthermore, clinical lineages have a higher proportion of antimicrobial resistance genes and there is evidence for substantial propagation of drug-resistant clades over time and geographic location (12, 14, 16). These major infection-associated lineages are now represented by hundreds of sequenced strains enabling experimental examination of phenotypes that are predicted to impact bacterial survival during infection. Our own work has also demonstrated a dichotomy between clinical and

environmental *S. marcescens* lineages strictly through comparison of the capsule polysaccharide (CPS) encoding locus and independent of more global genomic variation (17).

The CPS of *S. marcescens* is a critical fitness determinant during bloodstream infection (18). Like many encapsulated Enterobacterales species, the CPS of *S. marcescens* is encoded in a discrete genomic locus that exhibits extensive variability between isolates (17). Our comparison of capsule loci (KL) from clinical infection isolates determined that two KL clades were overrepresented among a cohort of >300 genomes and that strains from both of these groups, designated KL1 and KL2, produced sialylated CPS. Ketodeoxynonulonic acid (KDN) was the predominant sialic acid identified from polysaccharide preparations of KL1 and KL2 strains but a minor proportion of *N*-acetylneuraminic acid (Neu5Ac) was also detected. In addition to the two predominant clinical capsule types, smaller capsule clades associated with either clinical isolates or non-infection isolates were also defined, allowing for the comparison of strains belonging to each of these selected capsule clades. In this work, we sought to determine the infection characteristics of *S. marcescens* strains representing five different capsule clades using multiple model systems relevant to the infection niche.

RESULTS

Infectivity of *S. marcescens* isolates following bloodstream inoculation.

Capsule was determined to be an important fitness factor based on experiments using a single *S. marcescens* bacteremia clinical isolate belonging to clade KL1 (17, 18). In this study, we sought to compare *in vivo* survival characteristics of five *S. marcescens* strains assigned to different capsule clades. As an initial assessment of infection capability for isolates differentiated by capsule type, individual strains selected from clades KL1-KL5 (Table 1) were inoculated into the bloodstream of mice via tail vein injection (TVI) and bacterial survival was measured at 24 h post-injection. KL1 strain UMH9 stably colonized the spleen, liver, and kidneys in a manner consistent with previous results (19) (Fig. 1). However, significant variation in bacterial burdens

was observed among the strains in both the spleen and liver (Fig. 1A and 1B), with KL3 bacteremia isolate UMH7 consistently achieving the highest density in all tested organs. KL2 (gn773) and KL4 (UMH11) clinical bacteremia representatives were similarly elevated in spleen and liver bacterial burdens compared to KL1 and *S. marcescens* type strain ATCC 13880 (KL5), a pond water isolate, which exhibited a generally lower overall burden compared to most other strains. Although variability in the kidneys was higher than the other tested organs (Fig. 1C), the KL2 and KL5 strains trended towards lower colonization levels, and in some cases approached the limit of detection. Thus, while all tested *S. marcescens* strains, both clinical and non-clinical, were capable of infection in this model, significant organ-specific colonization differences are observed between strains of the five KL types.

Generation of acapsular mutant strains.

Before testing the contribution of CPS to infection for each KL type, acapsular mutants were first generated (Table 1). The strains selected from clades KL1, KL3, KL4, and KL5 were mutated such that the variable and clade specific region of each KL (CPS_v) (Fig. S1A) (17) was deleted and replaced with an insert fragment encoding kanamycin resistance. Attempts to construct an analogous CPS_v mutation in the KL2 strain were unsuccessful, despite multiple efforts using different mutagenic systems. As an alternative, a capsule-null phenotype was achieved in KL2 by disrupting the *neuB* gene encoding the sialic acid synthase within the CPS_v region of this strain, similar to a previously engineered capsule-null *neuB* mutant of KL1 strain UMH9 (17). Initial assessments of these five mutants demonstrated that the KL mutations disrupted high molecular weight capsule polysaccharide production, eliminated surface display of extracellular uronic acids, but did not prevent O-antigen production (Fig. S1). The only exception to these observations was KL5, which did not yield detectable CPS or O-antigen by either the wild-type or ΔCPS_v derivative stain under the tested culture conditions. Finally, a second acapsular KL1 derivative was generated that harbored a deletion of the entire capsule encoding

locus from the five-gene conserved region (*galU*, *galF, wza*, *wzb*, *wzc*) through the clade-specific variable locus (Fig. S1A). The purpose of this ΔKL1 mutant was to provide an isogenic background in which to express heterologous KL from other strains and, as expected, the ΔKL1 strain exhibited a significant loss of CPS production compared to the wild-type strain as determined by measuring extracellular uronic acids (Fig. 2A).

To confirm that CPS_v mutations were responsible for the loss of capsule and to generate mobilizable constructs for heterologous CPS production, the KL regions from each of the five selected strains were cloned into the bacterial artificial chromosome (BAC) pGNS-BAC1 (20). The constructs consisted of the five-gene conserved KL region, intergenic sequences upstream of *galU*, all clade-specific KL open reading frames and ranged from 15-23 kb in length (Table 1). Transformation of the pBAC-KL plasmids into their respective capsule mutant strains resulted in complete restoration of extracellular uronic acid production for strains KL1, KL2, KL3, and KL4 (Fig. 2A-D). Thus, the engineered pBAC-KL constructs are functional and sufficient to restore CPS production in their native strains. As expected, no significant change in uronic acids was observed when pBAC-KL5 was introduced into the KL5 ΔCPS_v mutant and all three tested strains had similarly low background levels (Fig. 2E).

Strain-specific limitations prevent heterologous capsule production.

The ability to express different capsule types in a single genetic background would provide a controlled system for testing the relative contribution of each CPS type to infection fitness. Therefore, pBAC-KL constructs were transformed into the UMH9 ΔKL1 strain and CPS production was first tested by quantitating uronic acids. None of the pBAC constructs harboring KL2-5 yielded significant increases in uronic acids compared to the ΔKL1 mutant control and only the pBAC-KL1 plasmid restored uronic acid detection (Fig. 3), as previously demonstrated (Fig. 2A). Total extracellular polysaccharides were next isolated from these strains and high molecular weight capsule material was visualized by SDS-PAGE. Consistent with the uronic acid assay results in

Figure 2, each of the pBAC-KL constructs was able to restore production of CPS when introduced into the native acapsular strains (Fig. 4). However, no CPS was detected when these same plasmids were present in the ΔKL1 strain. The lack of both extracellular uronic acids and high molecular weight polysaccharide from the heterologous pBAC-KL constructs in ΔKL1 demonstrates that CPS synthesis is precluded in this strain, despite the functionality of the BAC constructs in their cognate genetic backgrounds. These results strongly suggest that additional clade- or strain-specific elements are necessary for CPS synthesis and may be encoded outside the KL region as currently defined.

Capsule contributions to bacterial survival following bloodstream inoculation.

Since it was not feasible to assess the contribution of each CPS to infection independent of non-capsular genomic variation, we elected to determine the requirement for CPS within each KL type. First the relative fitness of capsule mutants was tested in comparison to wild-type parent strains via competition infections in the TVI bacteremia model. All tested KL types under these mixed inoculum parameters exhibited similar bacterial burdens in the spleen, kidneys, and liver of infected mice (Fig. S2). For each strain that was capable of CPS production *in vitro* (Fig. 4, Fig. S1), a significant competitive disadvantage in survival after 24 h was observed for mutants lacking capsular genes (Fig. 5A-D). For the KL4 strain, the fitness advantage provided by CPS was only significant for bacteria residing in the liver but showed a similar trend in the kidneys. Combined, these results indicate that capsule is important for bacterial survival during infection across the clinical *S. marcescens* isolates and capsular clades tested here. In contrast, the KL5 strain demonstrated no significant change in fitness in the absence of CPS_v genes (Fig. 5E). While this result was anticipated given the lack of CPS production associated with this strain, the question remains as to the functional significance for the six genes present in the ATCC 13880 KL5 CPS_v region (Fig. S1).

Given the lack of CPS production (Figs. 2 and 4) and a KL mutant infection phenotype by KL5 ATCC 13880 (Fig. 5E), it is not surprising that significantly lower bacterial burdens were observed for this strain compared to some the clinical isolates tested in Figure 1. However, no significant difference in organ colonization was observed between the KL1 clinical strain and KL5, despite the hypothesized survival advantage that would be afforded to KL1 by its sialylated CPS. To investigate this apparent discrepancy, infections were repeated for wild-type KL1 and KL5 strains with additional determinations of bacterial burden at 4 and 48 h post-inoculation. Consistent with earlier results, no significant difference between the two strains was observed after 24 h (Fig. 6). However, KL1 bacteria survived significantly better in all tested organs at 48 h post-inoculation compared to KL5 (Fig. 6A-C) and by at least one order of magnitude. Therefore, the KL5 strain is more susceptible to clearance and at an infection disadvantage over time compared to KL1. KL1 bacteria additionally expanded beyond the 24 h levels in both the liver and kidneys by 48 h, indicating that this strain is not only capable of enhanced survival in these organs but also replication.

The combined competition infection data indicate a decreased ability of acapsular mutants to withstand the antibacterial clearance mechanisms of the host. To further establish this conclusion, *S. marcescens* strains were exposed to human serum for 90 minutes followed by enumeration of viable bacteria. Each of the KL1-KL4 clinical isolates exhibited a CPS-dependent enhancement in serum resistance that was at least 6-fold greater than acapsular mutant derivatives while again, no significant difference in serum survival was observed between the KL5 strains (Fig. 7). Thus, serum resistance appears to be at least one mechanism by which the capsule of clinical strains provides a selective advantage to *S. marcescens*.

Requirement for capsule in a *S. marcescens* bacteremic pneumonia model.

Bloodstream infections frequently originate from localized infections that then disseminate and become systemic (21). During the processes of primary site colonization, dissemination, and organ colonization, bacteria may encounter different selective pressures compared to primary bacteremia in which organisms gain direct access to the bloodstream via an exogenous source such as a hypodermic needle or intravenous catheter. To address the need to characterize primary site infection and dissemination, we developed a bacteremic pneumonia model applicable to *S. marcescens* and based on a previously described *K. pneumoniae* infection model (22). Following retropharyngeal inoculation of wild-type and capsule mutant strain mixtures into C57BL/6J mice, robust colonization of the lungs was observed for all tested strain pairs at 24 hours post-inoculation (Fig. 8A). Furthermore, the spleen, kidneys, and liver were all colonized at this same time point (Fig. 8B-D) and to levels that approximated those observed in the primary bacteremia model (Fig. 1). Thus *S. marcescens* escape from the lungs occurs readily and results in stable organ colonization. The overall trends in bacterial burdens of the spleen, kidneys, and liver between this dissemination-dependent route and the direct TVI model were also similar for individual strains in that KL3 bacteria exhibited the highest density of infection followed by KL2 and KL4, then KL1 and KL5 (Fig. 1A-C and Fig. 8 B-D). Lastly, bacterial accumulation at systemic sites also correlated to primary lung bacterial density when assayed at the time of sacrifice (Fig. 8A) despite the inoculation of each animal with the same target dose. Together, these results further support the conclusion that significant variations exist between strains in their capacity to replicate and survive within local infection environments and that these variations occur both among the clinical isolates and isolates from non-clinical sources.

To define the requirement for capsule in secondary bacteremia, the relative recovery of capsule mutant and wild-type cells for KL1-5 strains was determined as a competitive index (CI). The four acapsular strains of clinical origin all demonstrated a severe competitive disadvantage compared to wild-type strains (Fig. 8E-H), with the mean recovery of capsule-deficient strains

being *ca*. 100-fold or less than wild-type for most organ and strain combinations. Thus, in both primary and secondary bacteremia models, capsule is a critical fitness factor across human-associated *S. marcescens*. Unexpectedly, a significant competitive disadvantage for the capsule mutant derivative of KL5 was also observed in the spleen, kidneys, and liver for this model (Fig. 8I). Given the contrast between these results with those of the same organ sites following TVI (Fig. 5E), the mutated KL5 capsular genes appear to play a role in bacterial survival during lung dissemination. This conclusion is further supported by the lack of a competitive disadvantage for the KL5 capsule mutants in the primary lung site. The only other tested strain that exhibited similar disparity between lung and distal organ CI was KL1; however, in this case the mean CI trended toward capsule-dependent lung fitness (*ca*. 8-fold disadvantage) and CPS is readily detected from KL1.

Sialylated CPS protect *S. marcescens* during macrophage interactions.

Previous work demonstrated that an acapsular derivative of KL1 strain UMH9 was internalized more readily by the U937 monocytic cell line compared to wild-type bacteria (17), resulting in the hypothesis that KL1 CPS has anti-phagocytic properties for *S. marcescens*. To determine whether CPS from other KL types also inhibited bacterial internalization, relative numbers of intracellular bacteria were measured in murine bone marrow-derived macrophages (BMDM). The proportion of viable intracellular capsular mutants was compared to wild-type bacteria at three time points following co-incubation with BMDM and subsequent treatment with gentamicin to kill extracellular bacteria (Fig. 9A). For both KL1 and KL2 sialylated capsule types, higher numbers of viable and internalized acapsular bacteria were recovered compared to wild-type relative to the inoculum and calculated as an internalization index. This imbalance resulted in a significant difference in the internalization index for both strains (Fig. 9B and C), establishing that both KL1 and KL2 CPS contribute to macrophage phagocytosis resistance. Furthermore, the trend toward higher intracellular non-encapsulated bacteria was consistent at all three time points

making it unlikely the observed differences were due to differential survival between strains. In contrast, none of the non-sialylated CPS KL types tested exhibited a significant difference in internalization under the same conditions, resulting in a neutral internalization index for KL3, KL4, and KL5 bacteria (Fig. 9D-F). The comparative lack of CPS-dependent phagocytosis resistance for the KL3 and KL4 clinical strains, in particular, suggests an important role for sialylated *S. marcescens* CPS in innate immune interactions and may be one contributing factor to the successful adaptation of these lineages to infection.

DISCUSSION

In this work, four *S. marcescens* strains isolated from human bloodstream infections and the type strain for this species were assayed for survival characteristics in conditions relevant to systemic infection. These strains were selected on the basis of their placement in five sequence-defined capsule clades and while all tested strains demonstrated an ability to infect mice using two different bacteremia models, significant differences in organ colonization were observed between them. Since strain-specific limitations prevented testing of individual CPS contributions in an isogenic background, it's not possible to attribute the observed strain-to-strain differences to capsule type alone and it's likely that mutiple factors contribute to the observed infection phenotypes. The biology underlying the inability of KL2-5 capsule gene clusters to yield CPS when introduced into KL1 bacteria is currently under investigation but is hypothesized to involve a regulatory component or a factor related to the compositional differences between CPS. Despite this technical limitation, capsule-dependent bacterial survival was demonstrated for all tested strains of clinical origin in human serum and both primary and secondary murine models of bacteremia. In contrast, the *S. marcescens* type strain ATCC 13880 was susceptible to human serum, did not produce CPS or O-antigen in culture, was cleared faster than a KL1 strain, and showed no role for capsule encoding genes during TVI bacteremia. However, the KL5 strain did exhibit a modest role for KL genes during or after dissemination from the lung. Since we have

been unable to detect CPS from cultured KL5 here or in previous reports (17), the basis for this KL5 mutant phenotype is currently unknown, but it's possible that the selective pressures associated with dissemination from the lung trigger KL5 CPS production via an unknown mechanism. What is clear from our experiments is that ATCC 13880 shows a lesser dependence on capsule during experimental infection compared to the clinical strains. Given the mounting genomic evidence separating the ATCC 13880 type strain from representative clinical lineages (12, 14, 15), it is perhaps unexpected that ATCC 13880 was generally capable of infectivity in both murine infection models. One contributing factor to this observation may be indicated by the overwhelming susceptibility of ATCC 13880 to human serum relative to the KL1-4 isolates. Since murine serum has been shown to lack the potent antibacterial capacity associated with human serum and serum complement (23-25), a lack of complement-mediated killing may be one means by which the murine models fail to capture all the selective pressures present in human bloodstream infections and it is possible that strains like ATCC 13880 may have lower infection potential in humans.

Among the tested strains only the CPS of KL1 and KL2 *S. marcescens* had a protective effect against BMDM internalization in this study. We hypothesize that the sialic acids associated with these strains, namely KDN and Neu5Ac (17), may therefore have a role in manipulating *Serratia*-macrophage interactions. While such interactions have yet to be demonstrated for *S. marcescens*, this hypothesis is supported by experimentally established roles for Neu5Ac-mediated modulation of innate immune cells in the literature (26-28). It's worth noting here that non-sialylated *S. marcescens* CPS also have a significant, but perhaps different, role in infection as demonstrated by the relative fitness of encapsulated and non-encapsuled clinical strains from the KL3 and KL4 clades. In our previous KL comparison, the KL1 and KL2 lineages had the greatest number of representatives within our tested genome cohort and were overwhelmingly comprised of infection isolates (17). In the context of the extensive *S. marcescens* genomic

species architechture recently published by Ono *et al*. (12), the UMH9 KL1 and gn773 KL2 strains tested in this work both segregate into clade 1. This is notable because clade 1, as defined by the authors, was also almost exclusively comprised of hospital associated or clinical isolates, had a high number of antimicrobial resistance alleles, and encoded a distinguishable set of accessory genes compared to other lineages. This association also goes beyond just the two clade 1 isolates tested in this work. Of the 215 strains identified as either KL1 or KL2 in our study, 188 were also included in the Ono study and strikingly, all 188 were assigned to the clade 1 lineage. This observation independently confirms our conclusion that KL1 and KL2 CPS are a differential component of this infection-adapted *S. marcescens* lineage and together suggest that sialylated CPS likely contribute to the niche-specific characteristics that provide these *S. marcescens* strains with a selective advantage during infection.

MATERIALS AND METHODS

Bacterial strains and culture conditions. The *S. marcescens* strains used in this study are listed in Table 1. *Escherichia coli* DH10B and *E. coli* DH5α were routinely used for cloning purposes. *E. coli* DH5α harboring helper plasmid pRK2013 (29) or strain BW29427 (B. Wanner, unpublished) cultured in 0.3 mM diaminopimelic acid were used as donor strains for conjugation. Bacteria were cultured in either LB medium (30) with or without 20 mM glucose or M9 (31) medium supplemented with 1 mM $MgSO_4$, 36 µM $FeSO_4$, 100 µM $CaCl_2$ and 20 mM glucose. Antibiotics for bacterial culture were used at the following concentrations: kanamycin, 50 µg/mL; hygromycin, 200 µg/mL; spectinomycin, 100 µg/mL; gentamicin, 10 and 20 µg/mL; and ampicillin, 100 µg/mL.

Generation of *S. marcescens* mutant strains. The oligonucleotide primers used for mutant construction and confirmation are listed in Table S1. *S. marcescens* ATCC 13880 ΔCPS_v::*nptII* and UMH7 ΔCPS_v::*nptII* mutant strains were constructed by recombineering as previously

described (18, 32). The neomycin phosphotransferase gene (*nptII*) from pKD4 (33) was PCR-amplified with oligonucleotides possessing 5′ sequence homology to ~50-bp of sequence targeted to the CPS_v region. Oligonucleotides SM_P1 and SM_P2 were used to amplify the mutant allele for subsequent deletion of 8,538-bp of the CPS_v sequence in KL5 ATCC 13880. Oligonucleotides SM_P3 and SM_P4 were used to amplify the mutant allele for a 10,021-bp deletion within the UMH7 KL3 CPS_v region. Electrocompetent ATCC 13880 or UMH7 harboring pSIM18 and pSIM19 (34), respectively, were transformed with DpnI-treated PCR products. Kanamycin-resistant transformants were genotyped by PCR and sequencing (SM_P5-P8), then cured of recombineering plasmids.

S. marcescens UMH11 and gn773 mutations were generated by allelic exchange using derivatives of suicide plasmid pTOX11 (35). For construction of the pTOX11 + UMH11 ΔCPS_v::*nptII* (pTOX17) suicide vector, *nptII* was PCR amplified from pKD4 with SM_P9 and SM_P10 possessing 5′ sequence homology to BVG89_RS04470, the first gene downstream of *wzc*, and BVG89_RS04510, the second to last gene within the UMH11 CPS_v locus, respectively. A 790-bp fragment containing 607-bp of the 3′ end of *wzc* and 120-bp of the 5′ end of the first CPS_v gene (BVG89_RS04470) was amplified with SM_P11 and SM_P12. A second fragment 789-bp in length containing 63-bp of the 3′ end of the last CPS_v gene BVG89_RS04510 and downstream sequence containing 676-bp of the 3′ end of BVG89_RS04515 was amplified with SM_P13 and SM_P14. The backbone of pTOX11 was amplified with SH_P15 and SH_P16 and digested with DpnI and XmaI (NEB) prior to assembly with HiFi Assembly (NEB). For generation of the pTOX11 + gn773 Δ*neuB*::*nptII* (pTOX16) suicide construct, a 792-bp *nptII* fragment from pDK4 was PCR amplified with SM_P17 and SM_P18 possessing 5′ sequence homology to the 3′ end of *neuA* (AWYA5_RS09505) including the start codon of *neuB* (AWYA5_RS09500) and the last three codons of *neuB* including the 5′ end of AWY15_RS09495, respectively. A 693-bp fragment containing the 3′ end of *neuA* and the start codon of *neuB* was amplified with SM_P19 and SM_P20. A second 730-bp fragment containing the last three codons of *neuB* and 721-bp of

the 5′ end of AWY15_RS09495 was amplified with SM_P21 and SM_P22. pTOX11 was amplified with SM_P23 and SM_P24 and subsequently digested with DpnI and XmaI prior to assembly.

The UMH9 ΔKL1 mutant was generated with a derivative of pTOX11$_{nptII}$ (17). To construct pTOX11$_{nptII}$ + UMH9 ΔKL1 (pTOX20) a 503-bp sequence located upstream 106-bp from the start codon of *galU* was amplified SM_P25 and SM_P26. A 490-bp product located 88-bp downstream of the stop codon of BVGRS_04590 was amplified with SM_P27 and SM_P28. SM_P29 and SM_P30 was used to amplify the pTOX11$_{nptII}$ backbone and was digested with DpnI and SacI prior to assembly.

All pTOX constructs were confirmed by sequencing (pTOX16; SM_P19 and SM_P22, pTOX17; SM_P11 and SM_P14, pTOX20; SM_P31 and SM_P32) prior to conjugation using donor strain BW29427. Allelic exchange was performed as previously described (35). Oligonucleotide pairs SM_P33 and SM_P34, SM_P35 and SM_P36, and SM_P37 and SM_P38 were used to confirm UMH11 ΔCPS$_v$::*nptII,* gn773 Δ*neuB*::*nptII*, and UMH9 ΔKL1 alleles by sequencing, respectively. Transconjugants were also assessed by PCR to ensure Mu phage was not transferred from the BW29427 donor strain (36).

Genetic complementation. For genetic complementation of capsule mutant strains, KL sequences were cloned into Gram-negative BAC vector pGNS-BAC (20). PCR, with addition of a secondary extension step, was performed to amplify both the entire KL and upstream intergenic region of each strains in two fragments; UMH9 KL1 with oligonucleotides SM_P39 and SM_P40 (11,531 bp) and SM_P41 and SM_P42 (11,531 bp); gn773 KL2 with oligonucleotides SM_P43 and SM_P44 (10,316 bp) and SM_P45 and SM_P46 (10,278 bp); UMH7 KL3 with oligonucleotides SM_P43 and SM_P47 (8,336 bp) and SM_P48 and SM_P49 (8,449 bp); UMH11 KL4 with oligonucleotides SM_P43 and SM_P50 (9,208 bp) and SM_P51 and SM_P52 (9,202 bp); ATCC 13880 KL5 with oligonucleotides SM_P43 and SM_P53 (7,657 bp) and SM_P54 and SM_P55 (7,770 bp). Amplified KL regions were cloned into HindIII-digested pGNS-BAC1 using

HiFi DNA Assembly and transformed into electrocompetent *E. coli* DH10B. Gentamicin-resistant transformants were screened by PCR: SM_P56 and SM_P57, pGNS-BAC1 + KL1; SM_P58 and SM_P59 and SM_P60 and SM_P61, pGNS-BAC1 + KL2; SM_P62 and SM_P63, pGNS-BAC1 + KL3; SM_P64 and SM_P65, pGNS-BAC1 + KL4; SM_P66 and SM_P67 pGNS-BAC1 + KL5; SM_P68 and SM_P69. Recombinant pGNS-BAC1 plasmids were purified by alkaline lysis and whole-plasmid sequences were determined (SNPsaurus). Tri-parental mating was performed at 37°C for 5 h to introduce pGNS-BAC constructs into *S. marcescens*. Bacteria were plated on LB agar containing ampicillin and gentamycin to select for loss of *E. coli* donors and the presence of pGNS-BAC1 plasmids.

Quantitation of uronic acids and polysaccharide analysis. Extracellular uronic acids of *S. marcescens* were measured using previously described methods (17, 37, 38). Measurements were based on a standard curve of glucuronic acid and normalized to culture optical density (600 nm). Isolation of *S. marcescens* extracellular polysaccharides was adapted from published methods (17, 39). Purified CPS and LPS were electrophoresed by SDS-PAGE and visualized as described previously (17).

Murine models of infection. Murine infections were performed in accordance with protocols approved by the University of Michigan Institutional Animal Care and Use Committee and were in accordance with Office of Laboratory Animal Welfare guidelines. Mid-log phase *S. marcescens* suspended in PBS were used as the inoculum. For mono-infections, male and female 7- to 8-week-old C57BL/6J mice (Jackson Laboratories) were infected via TVI with 0.1 mL suspensions containing a target dose of $5x10^6$ CFU. For competition infections, wild-type bacteria were mixed at a 1:1 ratio with an antibiotic-resistant mutant strain and delivered via TVI at a dose of $5x10^6$ total CFU. Mice were euthanized 24 h post-infection, unless otherwise specified, and the spleen, liver, and kidneys were harvested and homogenized. Bacterial counts of the inoculum (input) and

organ homogenates (output) were determined by plating serial dilutions on LB agar with or without antibiotics. The CI was determined by the following calculation: $(CFU_{mutant}/CFU_{wildtype})^{output}/(CFU_{mutant}/CFU_{wildtype})^{input}$.

For the bacteremic pneumonia model, mid-log phase bacteria were delivered by pipette (0.05 ml) to the retropharyngeal space of lightly anesthetized 7- to 8-week-old mice at a target dose of $1x10^7$ total CFU. Mice were euthanized 24 h post-infection and the spleen, liver, kidneys, and lung were harvested. Viable counts from the inoculum and organ homogenates were determined by serial dilutions plated on LB agar with and without antibiotics and used to calculate the CI as described above.

Serum resistance. Bacterial viability following a 90-minute exposure to 40% pooled human serum (Innovative Research) was determined as previously described (17).

Phagocytosis assays. Isolation and propagation of BMDM was performed using established protocols (40). Monocytes from the femur and tibia bone marrow of 7- to 8-week-old C57BL/6J mice were diluted to $1x10^6$ cells/mL in medium containing 15% L929 cell supernatant. At 7 days post-harvest, BMDM were dissociated from wells with ice-cold 2 mM EDTA in DPBS and collected by centrifugation. BMDM were seeded into 96-well flat bottom plates at $1x10^5$ cells/well and incubated at 37°C at 5% CO_2 for 24 h prior to inoculation with bacteria.

Bacteria were cultured overnight in M9 medium containing 20 mM glucose, washed in phosphate-buffered saline (PBS), and resuspended in an equal volume of DMEM containing 10% FBS. Wild-type and antibiotic resistant mutant strains were mixed in 1:1 ratio and added to BMDM at target MOI of 20. Plates were centrifuged briefly and incubated at 37°C for 60 min in 5% CO_2. Medium was aspirated and wells were washed with DPBS. DMEM containing 10% FBS and 100 µg/mL gentamicin was then added to wells followed by incubation for 30 min at 37°C in 5% CO_2. The gentamicin-containing medium was aspirated and wells were washed again with DPBS. For

time point zero, wells were incubated in 1% Saponin at 37°C for 10 min, mixed with 0.1 mL LB medium, then serially diluted and plated on LB agar plate with and without antibiotic for determination viable counts. All other wells were incubated in of DMEM containing 10% FBS and 10 µg/mL gentamicin until the time cell lysis and determination of viable counts. Internalization indices were calculated as described for CI with internalized bacteria substituting for the infection output parameter.

ACKNOWLEDGEMENTS

The authors would like to thank Mark Liles for kindly sharing the pGNS-BAC1 bacterial artificial chromosome plasmid and Caity Holmes for providing L929 cells and guidance regarding BMDM propagation.

FUNDING

This work was supported by Public Health Service award AI148767 to M. T. A. from the National Institutes of Health and AI134731 from the National Institutes of Health to H.L.T.M. and M.A.B. The funders had no role in study design, data collection and analysis, or preparation of the manuscript.

Table 1. *S. marcescens* strains and recombinant plasmids used in this study.

Name	Genotype/description	Clade	Reference
bacteria			
UMH9	wild-type	KL1	(18)
UMH9	ΔCPS$_v$::*nptII*	KL1	(17)
UMH9	ΔKL1	KL1	this study
gn773	wild-type	KL2	(16)
gn773	Δ*neuB*::*nptII*	KL2	this study
UMH7	wild-type	KL3	(18)
UMH7	ΔCPS$_v$::*nptII*	KL3	this study
UMH11	wild-type	KL4	(18)
UMH11	ΔCPS$_v$::*nptII*	KL4	this study
ATCC 13880	wild-type	KL5	American Type Culture Collection
ATCC 13880	ΔCPS$_v$::*nptII*	KL5	this study
plasmids			
pBAC-KL1	23.0-kb, 18-ORF insert encoding KL1	KL1	this study
pBAC-KL2	20.5-kb, 16-ORF insert encoding KL2	KL2	this study
pBAC-KL3	16.7-kb, 13-ORF insert encoding KL3	KL3	this study
pBAC-KL4	18.3-kb, 15-ORF insert encoding KL4	KL4	this study
pBAC-KL5	15.4-kb, 11-ORF insert encoding KL5	KL5	this study

FIGURE LEGENDS

Figure 1. **Organ colonization by *S. marcescens* strains following TVI bacteremia.** *S. marcescens* strains were inoculated into C57BL/6J mice (n=5) via TVI and bacterial colonization in spleen (A), liver (B), and kidneys (C) was determined by viable counts. Log transformed mean bacterial burdens are indicated by the solid lines. Statistical significance was assessed by ordinary one-way ANOVA with Tukey's multiple comparisons test: *, P < 0.05; **, P < 0.01; ***, P < 0.001; ****, P < 0.0001. The dotted line in panel C represents the highest value among samples that were at or below the limit of detection.

Figure 2. Generation of capsule-null mutations and genetic complementation via KL expression *in trans*. A-E**.** Capsule production by wild-type (WT) and capsule mutant *S. marcescens* strains representative of clades KL1-5 was measured by quantitating extracellular uronic acids and based on a standard curve of glucuronic acid. Statistical significance was assessed by unpaired t-test: **, P < 0.01; ***, P < 0.001; ****, P < 0.0001.

Figure 3. Lack of uronic acid production following introduction of heterologous KL sequences. Extracellular uronic acids were quantitated from the wild-type KL1 strain and a KL1 deletion mutant (ΔKL1) harboring the vector control plasmid (pGNS-BAC1) or plasmids containing the KL regions from each of five representative strains. Uronic acids were quantitated in comparison to a glucuronic acid standard curve. Statistical significance was determined using ordinary one-way ANOVA with Dunnett's multiple comparisons test against the negative control strain ΔKL1/pGNS-BAC1: Adj. P<0.0001, ****.

Figure 4. Lack of CPS production following introduction of heterologous KL sequences. A-E. Total bacterial polysaccharides from wild-type (WT) and capsule-null derivatives of strains representing five capsule clades were separated by SDS-PAGE and stained with alcian blue.

Capsule-null mutants harbored either the pGNS-BAC1 vector control plasmid or a recombinant plasmid with a cloned copy of the native KL. Recombinant KL plasmids were also expressed from a capsule-null mutant derivative of KL1 (ΔKL1). Pre-stained protein molecular weight standards (S) were electrophoresed on each gel with molecular weights shown in kDa.

Figure 5. Requirement for capsule among clinical strains during TVI bacteremia. A-E. CI for bacteria recovered from mixed strain competition TVI infections (24 h) in C57BL/6J mice. Solid lines represent the mean of log transformed values. Red outlined symbols indicate CI for which mutant bacteria were recovered at or below the limit of detection. Statistical significance was determined by one sample t-test with a hypothesized mean value of zero (dotted line), representing neutral fitness: *, $P < 0.05$; **, $P < 0.01$; ***, $P < 0.001$. S, spleen; K, kidney; L, liver.

Figure 6. Increased clearance of KL5 compared to KL1 bacteria following TVI bacteremia. C57BL/6J mice were inoculated with either KL1 or KL5 wild-type bacteria via the TVI route and bacterial burdens in the spleen (A), liver (B), and kidneys (C) were determined at the indicated time points. The mean of log transformed numbers of viable bacteria recovered are indicated by the bars and dashed lines denote the highest value among samples that were at or below the limit of detection. Statistical significance was assessed by unpaired t-test with Holm-Sidak multiple comparisons test: **, Adj. $P < 0.01$; ***, Adj. $P < 0.001$.

Figure 7. Capsules of clinical isolates protect from serum bactericidal activity. The survival of wild-type (WT) and acapsular (A) mutant strains was determined in the presence of 40% human serum after 90 minutes exposure relative to time zero with bars representing mean values (n=3). The dashed line indicates the limit of detection, where relevant. Statistical significance was assessed by Student's t-test: **, $P < 0.01$; ***, $P < 0.001$.

Figure 8. Requirement for capsule during bacteremic pneumonia. Combined wild-type and capsule mutant bacteria recovered from the lung (A), spleen (B), liver (C), and kidneys (D) of C57BL/6J mice following mixed strain competition infections (24 h). Solid lines represent the mean of log transformed viable bacteria and the dotted line indicates the highest value among samples that were at or below the limit of detection from kidneys. Differences in bacterial burdens between strains were assessed by one-way ANOVA with Tukey's multiple comparisons test: *, $P < 0.05$; **, $P < 0.01$; ***, $P < 0.001$; ****, $P < 0.0001$. E-I. CI comparing relative survival of capsule mutant and wild-type bacteria in lung (Lg), spleen (S), kidneys (K), and liver (L) for the infections shown in panels A-D. Symbols with red outlines denote CI from which capsule mutant strains were recovered at or below the limit of detection. Fitness defects were assessed by one-sample t-test against the hypothetical null value of zero (dotted lines) representing neutral fitness: *, $P < 0.05$; **, $P < 0.01$; ***, $P < 0.001$; ****, $P < 0.0001$.

Figure 9. Sialylated CPS protect *S. marcescens* from macrophage internalization. A. Schematic timeline for BMDM infection experiments. B-E. Murine BMDM were co-infected at a 1:1 ratio with wild-type and capsule mutant derivatives of each clade followed by enumeration of viable intracellular bacteria. The relative number of intracellular mutant to wild-type bacteria was calculated as an internalization index. Bars represent the mean of log transformed internalization indices and significant deviation from the hypothetical null value of zero representing equivalent internalization was determined by one-sample t-test: *, $P < 0.05$; **, $P < 0.01$.

REFERENCES

1. Wisplinghoff H, Bischoff T, Tallent SM, Seifert H, Wenzel RP, Edmond MB. 2004. Nosocomial bloodstream infections in US hospitals: analysis of 24,179 cases from a prospective nationwide surveillance study. Clin Infect Dis 39:309-17.
2. Sader HS, Streit JM, Carvalhaes CG, Huband MD, Shortridge D, Mendes RE, Castanheira M. 2021. Frequency of occurrence and antimicrobial susceptibility of bacteria isolated from respiratory samples of patients hospitalized with pneumonia in Western Europe, Eastern Europe and the USA: results from the SENTRY Antimicrobial Surveillance Program (2016-19). JAC Antimicrob Resist 3:117.
3. Antimicrobial Resistance Collaborators. 2022. Global burden of bacterial antimicrobial resistance in 2019: a systematic analysis. Lancet 399:629-655.
4. Antimicrobial Resistance Collaborators. 2022. Global mortality associated with 33 bacterial pathogens in 2019: a systematic analysis for the Global Burden of Disease Study 2019. Lancet 400:2221-2248.
5. Raymond J, Aujard Y. 2000. Nosocomial infections in pediatric patients: a European, multicenter prospective study. European Study Group. Infect Control Hosp Epidemiol 21:260-3.
6. Dessi A, Puddu M, Testa M, Marcialis MA, Pintus MC, Fanos V. 2009. *Serratia marcescens* infections and outbreaks in neonatal intensive care units. J Chemother 21:493-9.
7. Johnson A, Watson D, Dreyfus J, Heaton P, Lampland A, Spaulding AB. 2020. Epidemiology of *Serratia* bloodstream infections among hospitalized children in the United States, 2009-2016. Pediatr Infect Dis J 39:e71-e73.
8. Mahlen SD. 2011. *Serratia* infections: from military experiments to current practice. Clin Microbiol Rev 24:755-91.

9. Raymann K, Coon KL, Shaffer Z, Salisbury S, Moran NA. 2018. Pathogenicity of *Serratia marcescens* strains in honey bees. mBio 9:e01649-18.

10. Patterson KL, Porter JW, Ritchie KB, Polson SW, Mueller E, Peters EC, Santavy DL, Smith GW. 2002. The etiology of white pox, a lethal disease of the Caribbean elkhorn coral, *Acropora palmata*. Proc Natl Acad Sci U S A 99:8725-30.

11. Mah-Sadorra JH, Najjar DM, Rapuano CJ, Laibson PR, Cohen EJ. 2005. *Serratia* corneal ulcers: a retrospective clinical study. Cornea 24:793-800.

12. Ono T, Taniguchi I, Nakamura K, Nagano DS, Nishida R, Gotoh Y, Ogura Y, Sato MP, Iguchi A, Murase K, Yoshimura D, Itoh T, Shima A, Dubois D, Oswald E, Shiose A, Gotoh N, Hayashi T. 2022. Global population structure of the *Serratia marcescens* complex and identification of hospital-adapted lineages in the complex. Microb Genom 8:000793.

13. Williams DJ, Grimont PAD, Cazares A, Grimont F, Ageron E, Pettigrew KA, Cazares D, Njamkepo E, Weill FX, Heinz E, Holden MTG, Thomson NR, Coulthurst SJ. 2022. The genus *Serratia* revisited by genomics. Nat Commun 13:5195.

14. Matteoli FP, Pedrosa-Silva F, Dutra-Silva L, Giachini AJ. 2021. The global population structure and beta-lactamase repertoire of the opportunistic pathogen *Serratia marcescens*. Genomics 113:3523-3532.

15. Abreo E, Altier N. 2019. Pangenome of *Serratia marcescens* strains from nosocomial and environmental origins reveals different populations and the links between them. Sci Rep 9:46.

16. Moradigaravand D, Boinett CJ, Martin V, Peacock SJ, Parkhill J. 2016. Recent independent emergence of multiple multidrug-resistant *Serratia marcescens* clones within the United Kingdom and Ireland. Genome Res 26:1101-9.

17. Anderson MT, Himpsl SD, Mitchell LA, Kingsley LG, Snider EP, Mobley HLT. 2022. Identification of distinct capsule types associated with *Serratia marcescens* infection isolates. PLoS Pathog 18:e1010423.

18. Anderson MT, Mitchell LA, Zhao L, Mobley HLT. 2017. Capsule production and glucose metabolism dictate fitness during *Serratia marcescens* bacteremia. mBio 8:e00740-17.

19. Anderson MT, Brown AN, Pirani A, Smith SN, Photenhauer AL, Sun Y, Snitkin ES, Bachman MA, Mobley HLT. 2021. Replication dynamics for six Gram-Negative bacterial species during bloodstream infection. mBio 12:e0111421.

20. Kakirde KS, Wild J, Godiska R, Mead DA, Wiggins AG, Goodman RM, Szybalski W, Liles MR. 2011. Gram negative shuttle BAC vector for heterologous expression of metagenomic libraries. Gene 475:57-62.

21. Holmes CL, Anderson MT, Mobley HLT, Bachman MA. 2021. Pathogenesis of Gram-negative bacteremia. Clin Microbiol Rev 34:e00234-20.

22. Bachman MA, Breen P, Deornellas V, Mu Q, Zhao L, Wu W, Cavalcoli JD, Mobley HL. 2015. Genome-wide identification of *Klebsiella pneumoniae* fitness genes during lung infection. mBio 6:e00775.

23. Siggins MK, Cunningham AF, Marshall JL, Chamberlain JL, Henderson IR, MacLennan CA. 2011. Absent bactericidal activity of mouse serum against invasive African nontyphoidal *Salmonella* results from impaired complement function but not a lack of antibody. J Immunol 186:2365-71.

24. Marcus S, Esplin DW, Donaldson DM. 1954. Lack of bactericidal effect of mouse serum on a number of common microorganisms. Science 119:877.

25. Holmes CL, Smith SN, Gurczynski SJ, Severin GB, Unverdorben LV, Vornhagen J, Mobley HLT, Bachman MA. 2022. The ADP-heptose biosynthesis enzyme GmhB is a conserved Gram-negative bacteremia fitness factor. Infect Immun 90:e0022422.

26. Mandrell RE, Apicella MA. 1993. Lipo-oligosaccharides (LOS) of mucosal pathogens: molecular mimicry and host-modification of LOS. Immunobiology 187:382-402.

27. Carlin AF, Uchiyama S, Chang YC, Lewis AL, Nizet V, Varki A. 2009. Molecular mimicry of host sialylated glycans allows a bacterial pathogen to engage neutrophil Siglec-9 and dampen the innate immune response. Blood 113:3333-6.

28. Chang YC, Olson J, Beasley FC, Tung C, Zhang J, Crocker PR, Varki A, Nizet V. 2014. Group B *Streptococcus* engages an inhibitory Siglec through sialic acid mimicry to blunt innate immune and inflammatory responses *in vivo*. PLoS Pathog 10:e1003846.

29. Figurski DH, Helinski DR. 1979. Replication of an origin-containing derivative of plasmid RK2 dependent on a plasmid function provided in *trans*. Proc Natl Acad Sci U S A 76:1648-52.

30. Bertani G. 1951. Studies on lysogenesis. I. The mode of phage liberation by lysogenic *Escherichia coli*. J Bacteriol 62:293-300.

31. Miller JH. 1972. Experiments in Molecular Genetics. Cold Spring Harbor Laboratory, Cold Spring Harbor, N. Y.

32. Thomason LC, Sawitzke JA, Li X, Costantino N, Court DL. 2014. Recombineering: genetic engineering in bacteria using homologous recombination. Curr Protoc Mol Biol 106:1 16 1-39.

33. Datsenko KA, Wanner BL. 2000. One-step inactivation of chromosomal genes in *Escherichia coli* K-12 using PCR products. Proc Natl Acad Sci U S A 97:6640-5.

34. Datta S, Costantino N, Court DL. 2006. A set of recombineering plasmids for Gram-negative bacteria. Gene 379:109-15.

35. Lazarus JE, Warr AR, Kuehl CJ, Giorgio RT, Davis BM, Waldor MK. 2019. A new suite of allelic-exchange vectors for the scarless modification of proteobacterial genomes. Appl Environ Microbiol 85:e00990-19.

36. Ferrieres L, Hemery G, Nham T, Guerout AM, Mazel D, Beloin C, Ghigo JM. 2010. Silent mischief: bacteriophage Mu insertions contaminate products of *Escherichia coli* random

mutagenesis performed using suicidal transposon delivery plasmids mobilized by broad-host-range RP4 conjugative machinery. J Bacteriol 192:6418-27.

37. Blumenkrantz N, Asboe-Hansen G. 1973. New method for quantitative determination of uronic acids. Anal Biochem 54:484-9.

38. Favre-Bonte S, Joly B, Forestier C. 1999. Consequences of reduction of *Klebsiella pneumoniae* capsule expression on interactions of this bacterium with epithelial cells. Infect Immun 67:554-561.

39. Tipton KA, Rather PN. 2019. Extraction and visualization of capsular polysaccharide from *Acinetobacter baumannii*. Methods Mol Biol 1946:227-231.

40. Weischenfeldt J, Porse B. 2008. Bone marrow-derived macrophages (BMM): isolation and applications. CSH Protoc 2008:prot5080 doi: 10.1101/pdb.prot5080.

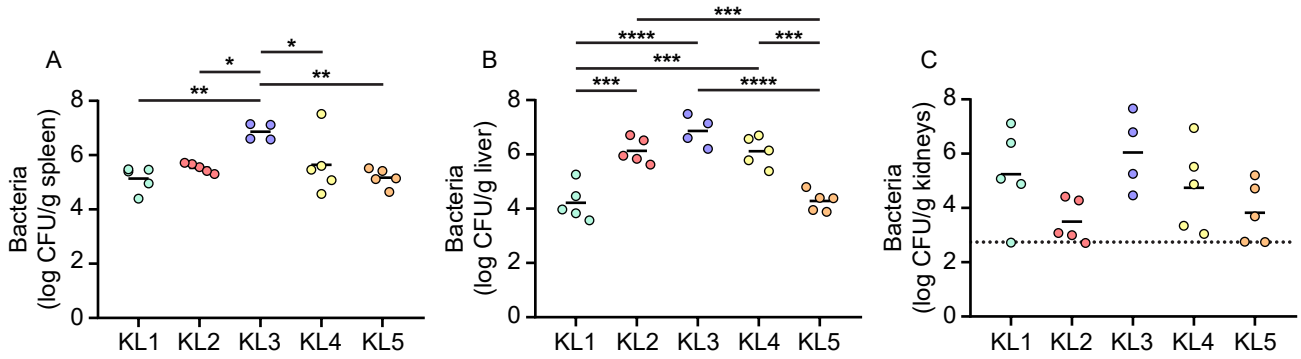

Figure 1. Organ colonization by *S. marcescens* strains following TVI bacteremia. *S. marcescens* strains were inoculated into C57BL/6J mice (n=5) via TVI and bacterial colonization in spleen (A), liver (B), and kidneys (C) was determined by viable counts. Log transformed mean bacterial burdens are indicated by the solid lines. Statistical significance was assessed by ordinary one-way ANOVA with Tukey's multiple comparisons test: *, $P < 0.05$; **, $P < 0.01$; ***, $P < 0.001$; ****, $P < 0.0001$. The dotted line in panel C represents the highest value among samples that were at or below the limit of detection.

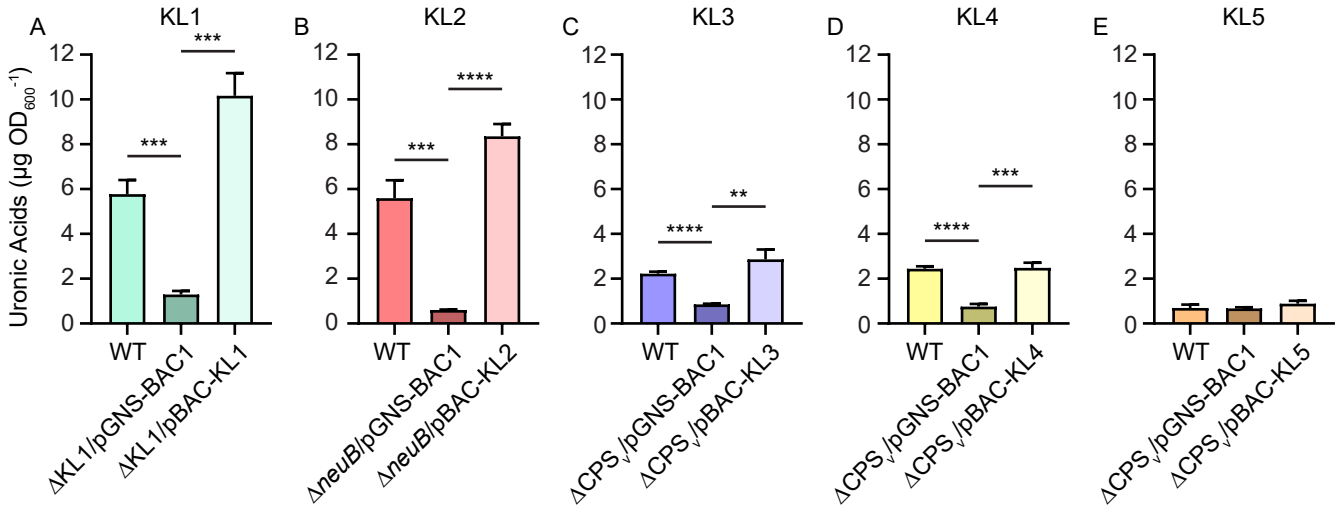

Figure 2. Generation of capsule-null mutations and genetic complementation via KL expression *in trans*. A-E. Capsule production by wild-type (WT) and capsule mutant *S. marcescens* strains representative of clades KL1-5 was measured by quantitating extracellular uronic acids and based on a standard curve of glucuronic acid. Statistical significance was assessed by unpaired t-test: **, P < 0.01; ***, P < 0.001; ****, P < 0.0001.

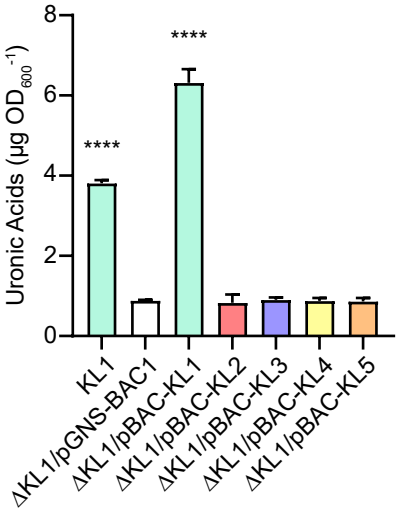

Figure 3. Lack of uronic acid production following introduction of heterologous KL sequences. Extracellular uronic acids were quantitated from the wild-type KL1 strain and a KL1 deletion mutant (ΔKL1) harboring the vector control plasmid (pGNS-BAC1) or plasmids containing the KL regions from each of five representative strains. Uronic acids were quantitated in comparison to a glucuronic acid standard curve. Statistical significance was determined using ordinary one-way ANOVA with Dunnett's multiple comparisons test against the negative control strain ΔKL1/pGNS-BAC1: Adj. P<0.0001, ****.

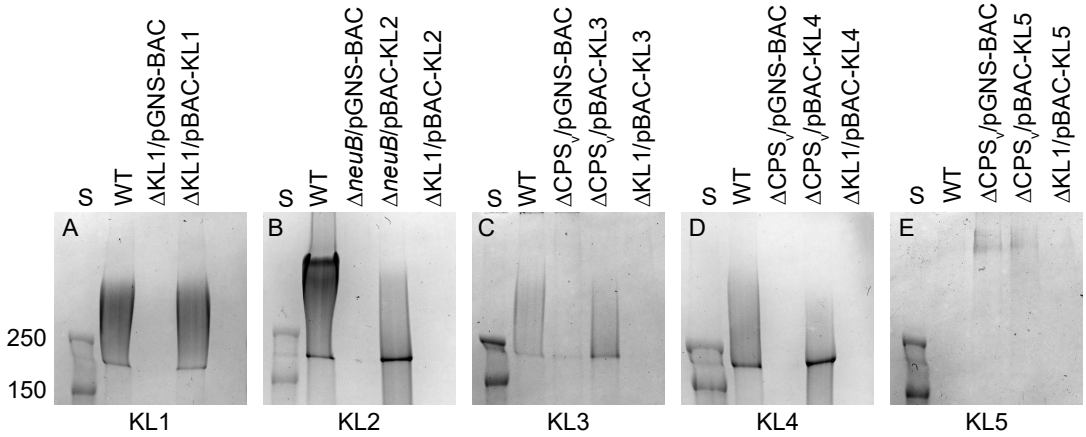

Figure 4. Lack of CPS production following introduction of heterologous KL sequences. A-E. Total bacterial polysaccharides from wild-type (WT) and capsule-null derivatives of strains representing five capsule clades were separated by SDS-PAGE and stained with alcian blue. Capsule-null mutants harbored either the pGNS-BAC1 vector control plasmid or a recombinant plasmid with a cloned copy of the native KL. Recombinant KL plasmids were also expressed from a capsule-null mutant derivative of KL1 (ΔKL1). Pre-stained protein molecular weight standards (S) were electrophoresed on each gel with molecular weights shown in kDa.

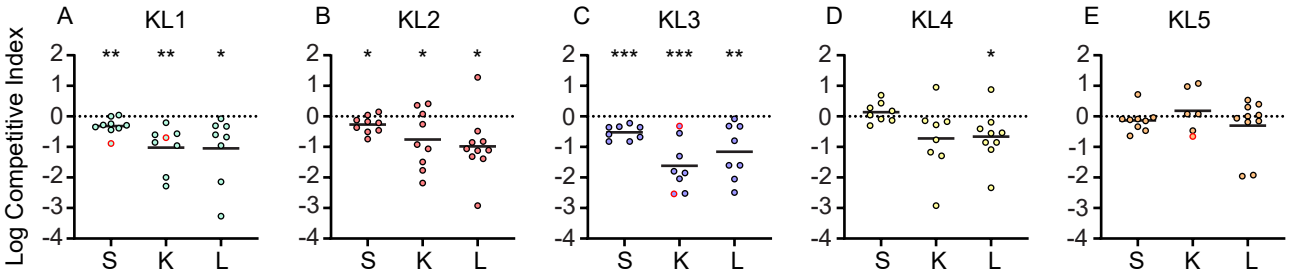

Figure 5. Requirement for capsule among clinical strains during TVI bacteremia. A-E. CI for bacteria recovered from mixed strain competition TVI infections (24 h) in C57BL/6J mice. Solid lines represent the mean of log transformed values. Red outlined symbols indicate CI for which mutant bacteria were recovered at or below the limit of detection. Statistical significance was determined by one sample t-test with a hypothesized mean value of zero (dotted line), representing neutral fitness: *, $P < 0.05$; **, $P < 0.01$; ***, $P < 0.001$. S, spleen; K, kidney; L, liver.

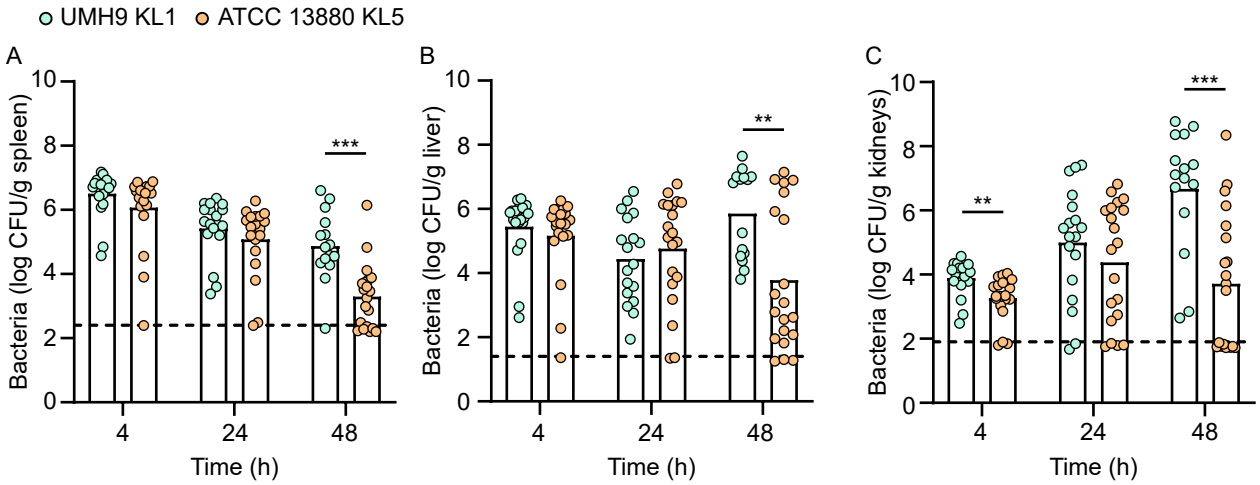

Figure 6. Increased clearance of KL5 compared to KL1 bacteria following TVI bacteremia. C57BL/6J mice were inoculated with either KL1 or KL5 wild-type bacteria via the TVI route and bacterial burdens in the spleen (A), liver (B), and kidneys (C) were determined at the indicated time points. The mean of log transformed numbers of viable bacteria recovered are indicated by the bars and dashed lines denote the highest value among samples that were at or below the limit of detection. Statistical significance was assessed by unpaired t-test with Holm-Sidak multiple comparisons test: **, Adj. P < 0.01; ***, Adj. P < 0.001.

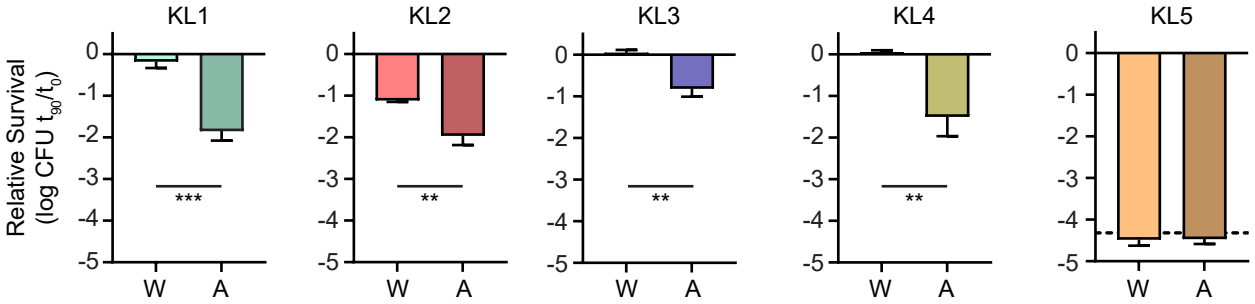

Figure 7. Capsules of clinical isolates protect from serum bactericidal activity. The survival of wild-type (WT) and acapsular (A) mutant strains was determined in the presence of 40% human serum after 90 minutes exposure relative to time zero with bars representing mean values (n=3). The dashed line indicates the limit of detection, where relevant. Statistical significance was assessed by Student's t-test: **, $P < 0.01$; ***, $P < 0.001$.

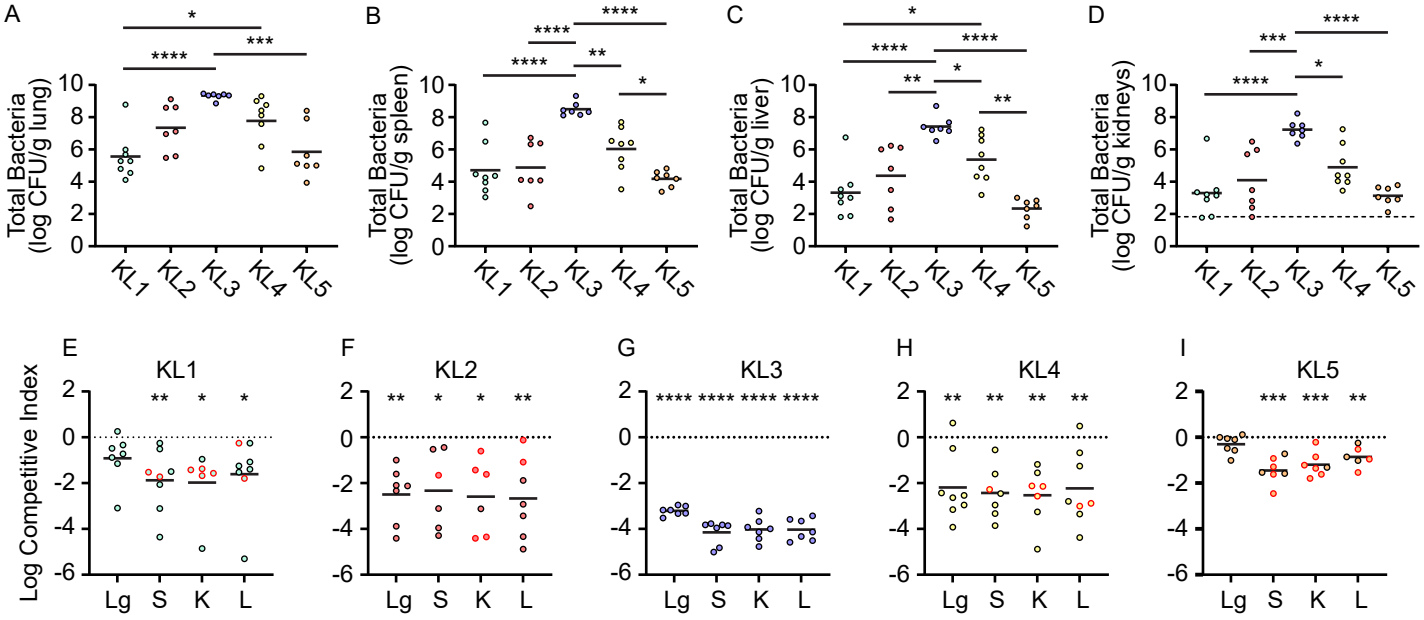

Figure 8. Requirement for capsule during bacteremic pneumonia. Combined wild-type and capsule mutant bacteria recovered from the lung (A), spleen (B), liver (C), and kidneys (D) of C57BL/6J mice following mixed strain competition infections (24 h). Solid lines represent the mean of log transformed viable bacteria and the dotted line indicates the highest value among samples that were at or below the limit of detection from kidneys. Differences in bacterial burdens between strains were assessed by one-way ANOVA with Tukey's multiple comparisons test: *, P < 0.05; **, P < 0.01; ***, P < 0.001; ****, P < 0.0001. E-I. CI comparing relative survival of capsule mutant and wild-type bacteria in lung (Lg), spleen (S), kidneys (K), and liver (L) for the infections shown in panels A-D. Symbols with red outlines denote CI from which capsule mutant strains were recovered at or below the limit of detection. Fitness defects were assessed by one-sample t-test against the hypothetical null value of zero (dotted lines) representing neutral fitness: *, P < 0.05; **, P < 0.01; ***, P < 0.001; ****, P < 0.0001.

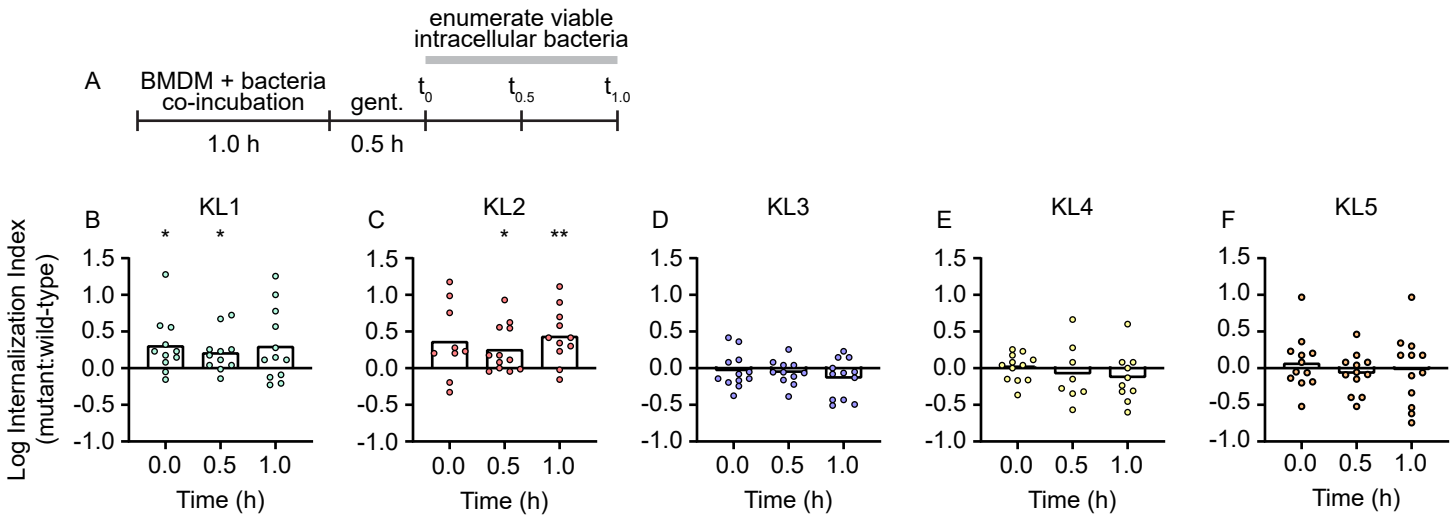

Figure 9. Sialylated CPS protect *S. marcescens* from macrophage internalization. A. Schematic timeline for BMDM infection experiments. B-E. Murine BMDM were co-infected at a 1:1 ratio with wild-type and capsule mutant derivatives of each clade followed by enumeration of viable intracellular bacteria. The relative number of intracellular mutant to wild-type bacteria was calculated as an internalization index. Bars represent the mean of log transformed internalization indices and significant deviation from the hypothetical null value of zero representing equivalent internalization was determined by one-sample t-test: *, $P < 0.05$; **, $P < 0.01$.